

# PLANS FOR A LINEAR PAUL TRAP AT RUTHERFORD APPLETON LABORATORY

D.J. Kelliher\*, S. Machida, C. Plostinar, C.R. Prior,  
 STFC Rutherford Appleton Laboratory, ASTeC

S.L. Sheehy,

JAI, Oxford & STFC Rutherford Appleton Laboratory, ASTeC

## Abstract

For over a decade, Linear Paul Traps (LPT) have been used in the study of accelerator beam dynamics. LPT studies exploit the similarity of the Hamiltonian with that of a beam in a quadrupole channel while having advantages in the flexibility of parameter choice, compactness and low cost. In collaboration with Hiroshima University, LPT research planned at STFC Rutherford Appleton Laboratory (RAL) in the UK aims to investigate a range of topics including resonance crossing, halo formation, long-term stability studies and space charge effects. Initially, a conventional quadrupole-based LPT will be built at RAL and used for a variety of experiments. In parallel, a design for a more advanced LPT that incorporates higher order multipoles will be pursued and later constructed. This multipole trap will allow non-linear lattice elements to be simulated and so broaden considerably the range of experiments that can be conducted. These will include the investigation of resonance crossing in non-linear lattices, a more detailed study of halo formation and the effect of detuning with amplitude. In this paper we report on progress made in the project to date and future plans.

## INTRODUCTION

In a linear Paul trap an rf electric field confines a non-neutral plasma transversely. The quadrupole symmetry of the electrodes focus and defocus the plasma in analogy with a bunch in a FODO channel. Longitudinally the plasma is trapped in a potential well created by applying DC voltages to end cap electrodes. The secular frequency of the plasma, equivalent to the cell tune in an accelerator, can be adjusted by varying either the frequency or voltage applied to the rf electrodes. Following a period of plasma confinement in which an experiment is performed, the plasma is extracted by lowering one of the DC voltages and sent to an external diagnostic.

For over a decade LPTs have been used in the study of accelerator beam dynamics both at Hiroshima University, Japan [1], [2] and at Princeton University, USA [3], [4]. At RAL, plans are advanced for the construction of an LPT based on the S-POD device at Hiroshima. As in S-POD, the device will consist of segmented cylindrical rod electrodes and the plasma (typically Argon) will be ionised in-situ using an electron gun. Diagnostics will include a Faraday

cup to measure the total number of ions and an MCP (Multi Channel Plate) screen imaged with a CCD camera (Fig.1).

Although initially a linear quadrupole trap will be constructed, the design should allow for the possibility of installing additional electrodes at a later date in order to add an octopole component. This would allow an investigation of halo formation in which the octopole term plays an important role [5]. It would also facilitate a study of detuning with amplitude during resonance crossing and when on-resonance in an extension of earlier work [6]. A more extensive list of proposed experiments can be found in ref. [7].

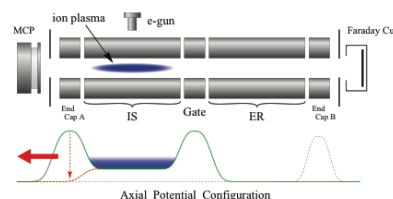


Figure 1: Schematic of S-POD showing the five segments used to create two trapping regions (IS: ion source region, ER: experimental region), and below, the potential well established by the DC voltages. As indicated by the arrows, by lowering the voltage applied to one set of end cap electrodes, the plasma moves towards an external diagnostic. The trap is about 20 cm in length and is operated at 1 MHz. Image courtesy of H. Okamoto and his group.

## QUADRUPOLE TRAP DESIGN

### Basic Design Parameters

The potential in the transverse plane in a LPT with quadrupole symmetry is given by

$$\Phi(x, y, t) = (U - V_0 \cos(ft)) \left( \frac{x^2 - y^2}{2r_0^2} \right) \quad (1)$$

where  $U$  is the DC potential applied to the end cap electrodes,  $V_0$  is the rf voltage of frequency  $f$  and  $r_0$  is the trap radius (i.e the radius that inscribes the trap electrodes). Making the following transformations

$$\begin{aligned} a_x &= a_y = \frac{4qU}{mr_0^2 f^2} \\ q_x &= -q_y = \frac{2qV_0}{mr_0^2 f^2} \\ \xi &= ft/2 \end{aligned}$$

\* David.Kelliher@stfc.ac.uk

it follows that the transverse equation of motion in this potential for a particle of charge  $q$  and mass  $m$  is given by the Mathieu differential equation

$$\frac{d^2u}{d\xi^2} + (a_u - 2q_u \cos(2\xi))u = 0 \quad (2)$$

where  $u = x, y$ . The resulting ion trajectories are subject to a rapid micromotion at the frequency of the rf and a lower frequency secular motion (analogous to the betatron motion in an accelerator) determined by the shape of the confining pseudopotential. As derived in ref. [1], assuming negligible collective effects, the secular motion in terms of phase advance per rf period (or "cell") can be written as follows

$$\sigma_0 = \frac{2\sqrt{2}qgV_0}{\pi^2m} \left( \frac{1}{fr_0} \right)^2 \quad (3)$$

where  $g$  is a function of the ratio of signal duration  $d$  and wavelength  $\lambda$  assuming a piecewise constant waveform (for the rest of this analysis, following ref. [1], we assume  $d/\lambda = 0.25$  in which case  $g \approx 0.712$ ). Note - the transverse tunes in the two planes can be split by applying different voltage amplitudes to each pair of electrodes. Assuming two of the parameters  $V_0, r_0$  and  $f$  are fixed by other considerations, this equation allows the remaining parameter to be set to obtain a desired phase advance.

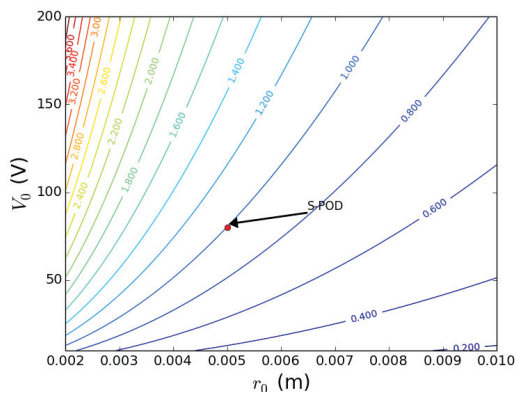


Figure 2: Contours showing rf frequency labelled in MHz as function of voltage and trap radius where the phase advance is set at  $\pi/2$ . The S-POD case is indicated.

As shown in [1], the maximum ion density that can be stored is proportional to the voltage. A voltage of about 80 V allows a sufficiently high ion intensity for collective effects to be significant (up to  $10^9$  ions can be stored in S-POD) while being practicable from an electronics point of view. The contours in Fig. 2 show the rf frequency required to obtain a phase advance of  $\pi/2$  (i.e. in the middle of the stability region) in terms of  $V_0$  and  $r_0$ . In the case of S-POD, the chosen configuration is a combination of 1 MHz rf frequency, 80 V and a trap radius of 5 mm.

The rf amplifier that will be used in the case of the LPT at RAL can produce frequencies from the  $\sim 100$  kHz range up to 2 MHz. A higher frequency is advantageous from

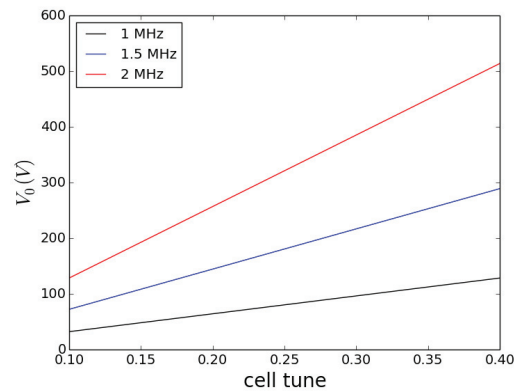


Figure 3: Required voltage as a function of cell tune for the case of 1 MHz, 1.5 MHz and 2 MHz rf. The trap radius  $r_0$  is fixed at 5 mm.

the point of view of plasma lifetime simply because more rf oscillations occur in a given time, in effect allowing the study of longer beam lines. As can be seen from Eqn. 3 (and in Fig. 2), a doubling in the frequency would require the trap radius (and the rod radii as shown below) to be halved to preserve the  $\pi/2$  phase advance at 80V.

Alternatively, keeping the radius fixed but increasing the rf frequency by a factor, requires the voltage to be raised by the square of the factor. As is clear in Fig. 3, the cell tune range that can be accessed at higher rf frequencies will then depend on the maximum voltage allowed by the electronics.

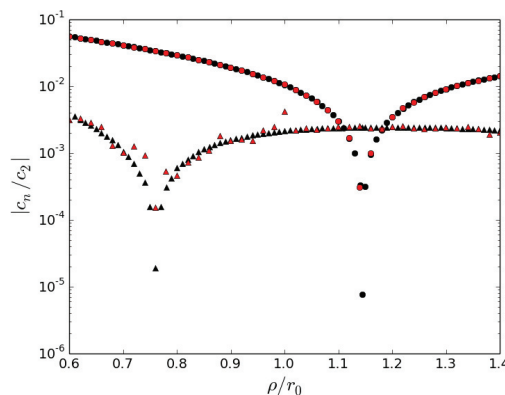


Figure 4: Normalised multipole coefficients  $c_6/c_2$  (circles) and  $c_{10}/c_2$  (triangles) as a function of the ratio of the electrode radius  $\rho$  and trap radius  $r_0$ . The harmonics were calculated 2 mm from the trap axis with  $r_0 = 5$  mm. 2D (black) and 3D (red) solvers were used to solve the Laplacian using Mathematica [8] and CST [9], respectively.

### Rod Radius and Alignment

It is reasonable to solve the electrostatic case since at  $\sim 1$  MHz, the size of the device is much smaller than the rf wavelength. In this paper we further reduce the problem by simply looking at a transverse slice through the plasma trap, ignoring longitudinal effects for now. The Laplacian

can be solved using the finite element method. Dirichlet boundary conditions corresponding to the rf voltages are imposed on each rod circumference. The external boundary is arbitrarily chosen - its effect is negligibly small [10]. Since the device has cylindrical symmetry, it makes sense to write the potential as the sum of multipoles

$$\psi(r, \theta) = \sum_{n=1}^{\infty} c_n \left(\frac{r}{r_0}\right)^n \cos(n\theta) \quad (4)$$

By taking the Fast Fourier Transform (FFT) of  $\psi$  evaluated along a circle around the trap axis, the multipole coefficients  $c_n$  can be found at a particular radius. The symmetry of the quadrupole trap case means that, in the ideal case, only every four harmonics are allowed, the first two being  $c_6$  (dodecapole) and  $c_{10}$  (20-pole).

Figure 4 shows how the first two allowed multipole components vary with the ratio of rod and trap radii. As a consistency check, the Laplacian was solved using 2D and 3D solvers. The minimum normalised dodecapole component  $c_6/c_2$  and 20-pole  $c_{10}/c_2$  are found at radius ratios 1.145 and 0.76, respectively. These results are in agreement with a semi-analytic approach [10], [11] and measurements [12]. Rather than choose the ratio which minimises a single multipole, it has been proposed by several authors to instead offset  $c_6$  against  $c_{10}$ . Depending on the details, this strategy leads variously to radius ratios of 1.11 [11] and 1.126-1.13 [13].

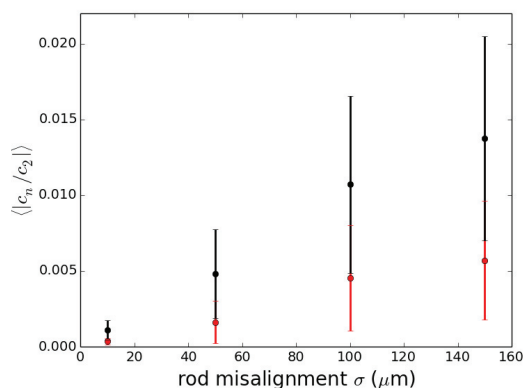


Figure 5: Mean normalised multipole coefficients  $c_3$  (black) and  $c_4$  (red) as a function of the magnitude of rod misalignment. The ratio of the rod to trap radius was set to 1.145 in order to minimise the dodecapole component. A set of 50 rod misalignments with Gaussian distribution truncated at 3 standard deviations was applied. The error bars represent the standard deviation of the results. The calculation was carried out, in 2D, 2 mm from the trap axis using Mathematica.

Transverse misalignment of the rods introduce multipole terms of all orders. The results of a 2D calculation, for the significant sextupole and octopole components, are shown in Fig. 5. A tolerable magnitude for each multipole term, which will set the required alignment accuracy, has yet to be established. For now it can be noted that in S-POD, where

the misalignment is of the order 50-100 microns [14], the effect of non-linearities can be observed [6].

## MULTIPOLE TRAP

By breaking the quadrupole symmetry additional multipole terms can be introduced without increasing the number of rods. For example, sextupole can be added by rotating one opposing pair of electrodes about the trap axis [15] and octopole by using pairs of rods with differing radii [1], [16]. However, in such schemes the level of multipole in comparison with the quadrupole term is fixed by the chosen geometry.

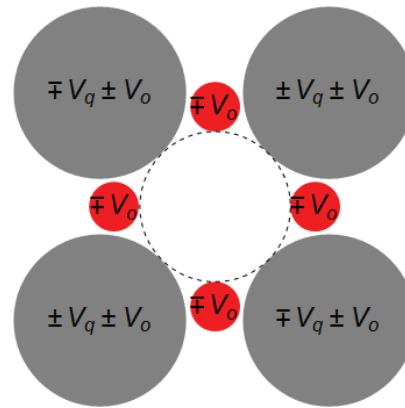


Figure 6: Cross-section of a quad-octupole trap. The polarity of the voltages applied to the quadrupole rods (grey) and the additional sub-rods for octopole (red) are shown.

A quadrupole trap with four additional sub-rods to create an octopole term (herein dubbed a "quad-octupole trap"), as proposed in [1], allows the desired flexibility (see Fig. 6). The quadrupole and octopole potentials can be independently set by applying voltages  $V_q$  and  $V_o$  to the appropriate set of electrodes. As shown in ref. [1], adjusting  $V_o$  leads to a variation in  $c_4$  and  $c_8$  while leaving  $c_6$  and  $c_{10}$  unaffected.

LPTs with identical, symmetrically arranged parallel rods have been constructed, with the purpose of exciting a single multipole [17]. The optimal rod radii for such single multipole traps are listed exhaustively in ref. [18]. On the other hand, the optimal radius is less clear in the case of a trap designed to excite more than one multipole.

## FUTURE PLANS

It is envisaged that a LPT will be designed and constructed at RAL in the next 12 months with commissioning to begin shortly thereafter. The work presented here is the first step in modelling efforts that will inform the design. A more comprehensive study will be carried out using CST to investigate longitudinal effects and, for example, errors arising from non-parallel rods.

## ACKNOWLEDGMENT

We would like to acknowledge the invaluable contribution of H. Okamoto and his group at Hiroshima University.

## REFERENCES

- [1] H. Okamoto, Nucl. Instr. Meth. A 485 (2002) 244-254.
- [2] R. Takai et al., Nucl. Instr. and Meth. A 532 (2004) 508-512.
- [3] R.C. Davidson, Nucl. Instr. and Meth. A 464 (2001) 502-511.
- [4] E.P. Gilson et al., Laser Part. Beams 21 (2003) 549-552.
- [5] G. Franchetti et al., Phys. Rev. ST Accel. Beams 13, 114203 (2010).
- [6] K. Moriya et al., Phys. Rev. ST Accel. Beams 18, 034001 (2015).
- [7] D.J. Kelliher et al., "Study of Beam Dynamics in Linear Paul Traps", Proc of HB2014, East Lansing, MI, USA, 85 (2014).
- [8] Mathematica website: <http://www.wolfram.com>
- [9] CST Studio: <http://www.cst.com>
- [10] D.R. Denison, J. Vacuum Sci. Technol. 8 (1971) 266.
- [11] J. Schulte, P.V. Shevchenko and A.V. Radchik, Rev. Sci. Instrum., 70(9), (1999) 3566-3571.
- [12] I.E. Dayton, F.C. Shoemaker and R.F. Mozley, Rev. Sci. Instrum., 25 (1954) 485.
- [13] D.J. Douglas, A.N. Kononkov, Rapid Commun. Mass Spectrom. 16(15) (2002) 1425-1431.
- [14] H. Okamoto, private communication.
- [15] N.V. Kononkov et al., J. Am. Soc. Mass Spectrom 17 (2006) 1063-1073.
- [16] M. Sudakov, D.J. Douglas, Rapid Commun. Mass Spectrom. 17 (2003) 2290-2294.
- [17] K. Okada et al., Phys. Rev. A 75, (2007) 033409.
- [18] A.N. Kononkov, D.J. Douglas, N.V. Kononkov, Int. J. Mass Spectrom. 289 (2010) 144-149.